Supplementary Material

Microfluidic nano-scale qPCR enables ultra-sensitive and quantitative detection of SARS-CoV-2

Xin Xie [1], Tamara Gjorgjieva [2,3], Zaynoun Attieh [1], Mame Massar Dieng [2], Marc Arnoux [4], Mostafa Khair [4], Yasmine Moussa [1], Fatima Al Jallaf [2,3], Nabil Rahiman [1], Christopher A. Jackson [5], Lobna El Messery [6], Khristine Pamplona [6], Zyrone Victoria [6], Mohammed Zafar [6], Raghib Ali [3], Fabio Piano [1,5], Kristin C. Gunsalus [1,3,5,*] and Youssef Idaghdour [2,3,*]

[1] Center for Genomics and Systems Biology, New York University Abu Dhabi, PO Box 129188, Abu Dhabi 51133, UAE
[2] Program in Biology, Division of Science, New York University Abu Dhabi, PO Box 129188, Abu Dhabi 51133, UAE
[3] Public Health Research Center, New York University Abu Dhabi, PO Box 129188, Abu Dhabi 51133, UAE
[4] Core Technology Platforms, New York University Abu Dhabi, PO Box 129188, Abu Dhabi 51133, UAE
[5] Department of Biology and Center for Genomics and Systems Biology, New York University, New York, NY 10003, USA
[6] Proficiency Healthcare Diagnostics, Electra Street, Abu Dhabi 51133, UAE
* Correspondence: kcg1@nyu.edu (K.C.G); youssef.idaghdour@nyu.edu (Y.I.)

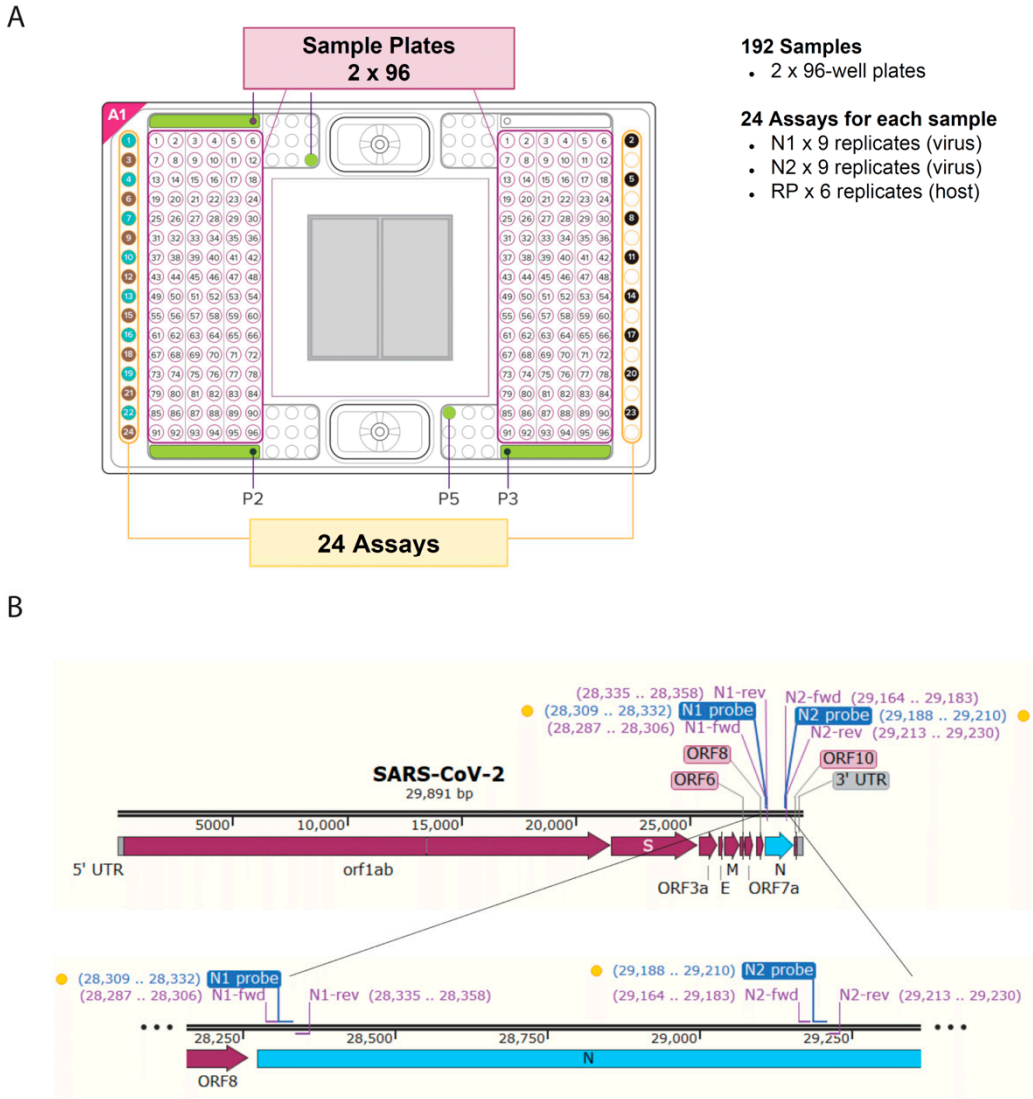

Figure S1. Microfluidic chip layout and N gene probes. (A) The 192x24 microfluidic chip can analyze 192 samples (from two 96-well microtiter plates) against 24 assays. In our experimental design, each sample was analyzed with 9 replicates each of the N1 and N2 (viral N gene) assays and 6 replicates of the RP (human gene) assay. (B) Schematics showing the locations of the PCR primers and Taqman probes for the N1 and N2 assays on the SARS-CoV-2 genome.

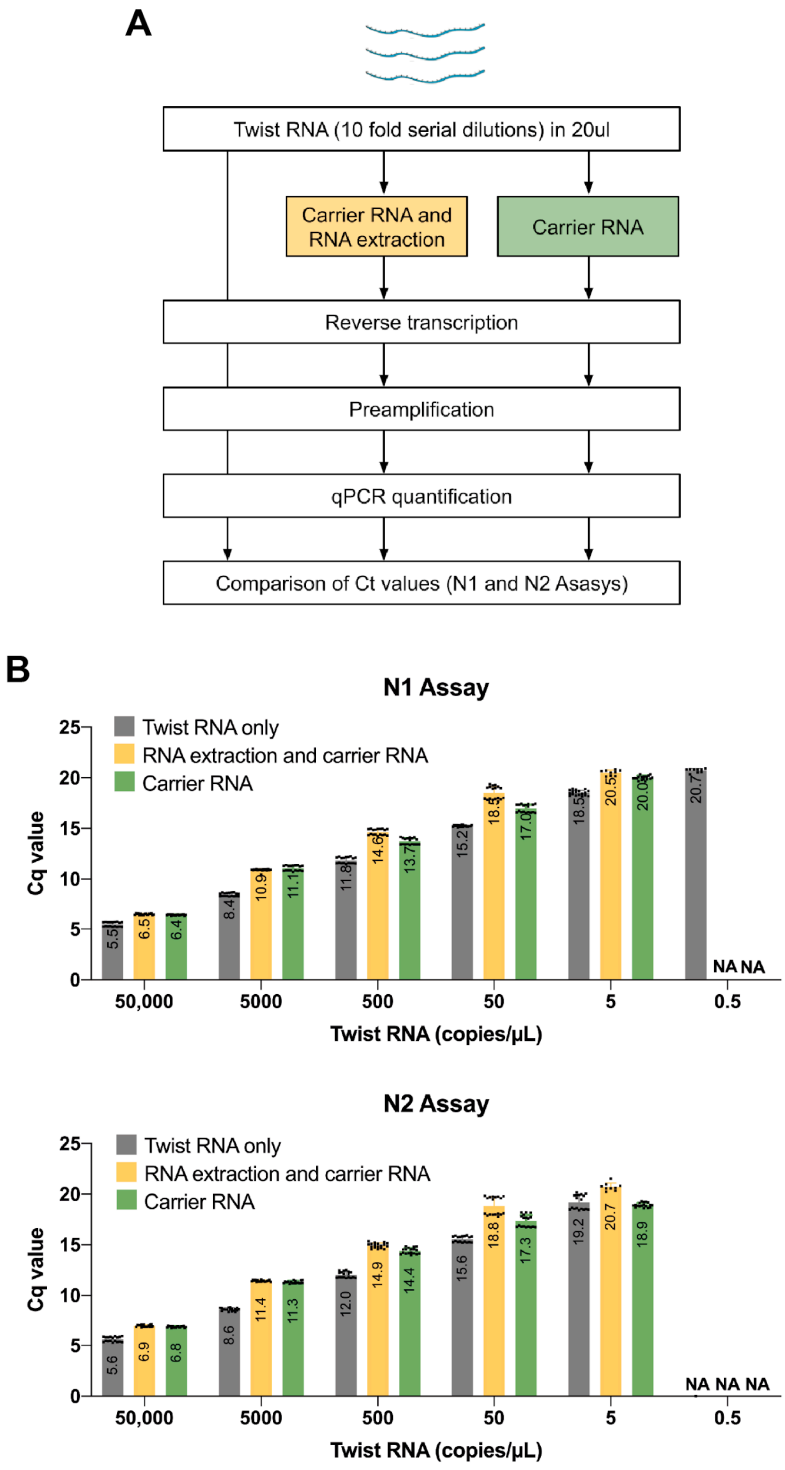

Figure S2. Detection limit with RNA extraction step and the effect of carrier RNA. Workflow for the analysis of serially diluted Twist RNA only, Twist RNA with an RNA extraction step in presence of carrier RNA or Twist RNA with the direct addition of carrier RNA. Data show the mean ± SD of valid Cq values from 18 replicates for each concentration (2 biological replicates with 9 technical replicates each).

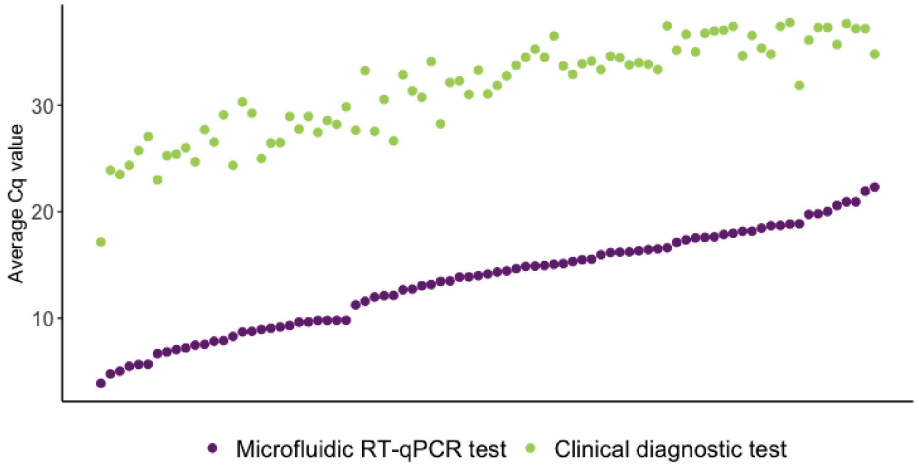

Figure S3. Consistency in Cq value ranking between the microfluidic RT-qPCR and the clinical diagnostic method. Plot comparing the ranked Cq values obtained from the microfluidic RT-qPCR test and the Cq value from the corresponding samples in the clinical diagnostic test. The Cq value is an average of the ORF1 and N gene assay for the clinical diagnostic test, and of the N1 and N2 assay for the microfluidic test.

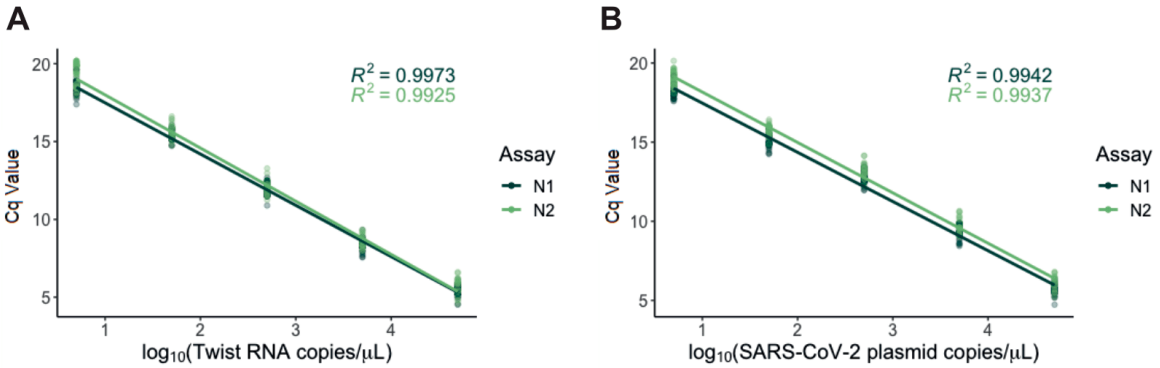

Figure S4. Linear regression of Cq values vs. copy number of serially diluted positive controls shows highly reproducible detection of SARS-CoV-2 across five orders of magnitude. Plots of Cq values vs. copy numbers of serially diluted positive controls show a strong log linear relationship ranging from 5 to 50,000 copies/µl for both N1 and N2 assays (with preamplification). (A) Synthetic RNAs (Twist RNA) and (B) SARS-CoV-2 plasmid. Data points show 18 replicates at each concentration. R^2, coefficient of variation.

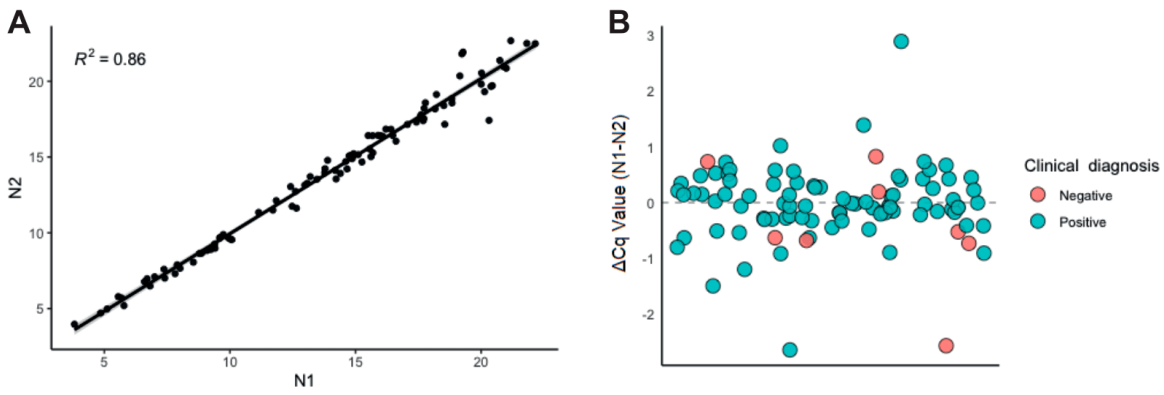

Figure S5. Comparison of detection performance between N1 and N2 assays. (A) Correlation between Cq values of the N1 and N2 assays (R^2 = 0.86, Kendall's rank correlation). (B) Scatter plot of the differences in Cq values between the N1 and N2 assays (Δ Cq (N1-N2)) in the Pos_Pos and Neg_Pos samples.